RUBIDIAN MICROCLINE FROM RED CROSS LAKE, NORTHEASTERN MANITOBA

PETR ČERNÝ; HORST PENTINGHAUS and JOSEPH J. MACEK

ČERNÝ, PETR; PENTINGHAUS, HORST and MACEK, JOSEPH J., 1985: Rubidian microcline from Red Cross Lake, northeastern Manitoba. *Bull. Geol. Soc. Finland 57, Part* 1—2, 217—230.

Dark grey, slightly perthitic and grid-twinned to non-perthitic and Baveno-twinned, near-maximum rubidian microcline occurs in sheared dikes of pollucite-bearing pegmatites at Red Cross Lake, northeastern Manitoba. The composition of the most rubidium-rich sample, free of mineral inclusions on optical microscopic scale, is $\mathrm{Or}_{70.3}\mathrm{Ab}_{11.4}\mathrm{An}_{0.4}\mathrm{Rb\text{-}f}_{16.9}\mathrm{Cs\text{-}f}_{0.9}\mathrm{Tl\text{-}f}_{0.05}$; the potassic phase of the perthite is close to $\mathrm{Or}_{76.5}\mathrm{Ab}_{3.9}\mathrm{An}_{0.2}\mathrm{Rb\text{-}f}_{18.4}\mathrm{Cs\text{-}f}_{1.0}\mathrm{Tl\text{-}f}_{0.05}$. Unit cell dimensions are a 8.6373(7), b 12.9691(5), c 7.2264(6)Å, α 90.588(5)°, β 116.002(5)°, γ 87.842(5)°, V 727.01(13)Å^3; triclincity 0.93; α 1.518—1.520, β 1.522—1.524, γ 1.525—1.526, (—)2V 76—80°, X' (001) 19—21°, X' (010) 7—8°; Euler angles $\Phi = +74°$, $\Psi = 95.5°$, $\Theta = 72.5°$; D(meas.) 2.612, D(calc.) 2.614; characteristic IR absorption bands at 15.455 and 18.585 μm. This rubidian microcline is the most rubidium-rich natural feldspar described to date. Its properties support the conclusion that high (Rb,Cs) contents may retard ordering in K-feldspar but are not a primary control of triclinization. Available data on K-feldspars show no consistent correlation between the highest Rb-contents and specific structural states in individual pegmatites.

Key words: rubidium, microcline, pegmatite, Manitoba.

Petr Černý: Department of Earth Sciences, University of Manitoba, Winnipeg, Manitoba, Canada R3T 2N2.

Horst Pentinghaus: Kernforschungszentrum Karlsruhe GmbH, 7500 Karlsruhe 1, Federal Republic of Germany.

Joseph J. Macek: Manitoba Department of Energy and Mines, Winnipeg, Manitoba, Canada R3C 4E3.

Introduction

Potassium feldspars enriched in rubidium, and with elevated contents of cesium, commonly occur in complex granitic pegmatites. It is particularly the extremely fractionated, pollucite-bearing pegmatite type enriched in Li, Rb, Cs, Be, Sn, Ta, F (and P, B) in which the Rb and Cs contents of K-feldspar reach maximum values: Varuträsk (3.3 wt.% $\mathrm{Rb_2O}$, and 0.6 wt.% $\mathrm{Cs_2O}$; Adamson 1942), Kola Peninsula (4.1 wt.% $\mathrm{Rb_2O}$ and 0.5 wt.% $\mathrm{Cs_2O}$; Gordiyenko and Kamentsev 1967), Lower Tanco (4.81 wt.% $\mathrm{Rb_2O}$ and 0.48 wt.% $\mathrm{Cs_2O}$; Ferreira 1984), and Tanco (3.61 wt.% $\mathrm{Rb_2O}$ and 0.48 wt.% $\mathrm{Cs_2O}$; unpubl. data of P. Č.). Occurrences of K-feldspars with Rb_2O contents in the range of 1.0—2.5 wt.% are much more common (*e.g.*, Foord 1976, Černý *et al.* 1981, Ucakuwun 1982, Anderson 1984, Lopes Nunes 1973, and other papers quoted in this last reference).

In summer 1981 one of us (P. Č.) collected samples of microcline in pegmatites at Red Cross Lake in Manitoba, known for the occurrence of Rb-rich lithium micas (Jambor and Potter 1967). One of the samples proved to contain 5.45 wt.% Rb_2O which is, to the best of our knowledge, the highest Rb_2O content found so far in a natural K-feldspar. Because of this exceptionally high Rb content, and because of a general lack of data on the physical properties of Rb-rich microclines (Gordiyenko's 1964 data refer to microclines with a maximum of 1.53 wt.% Rb_2O), two samples were selected for a more detailed study.

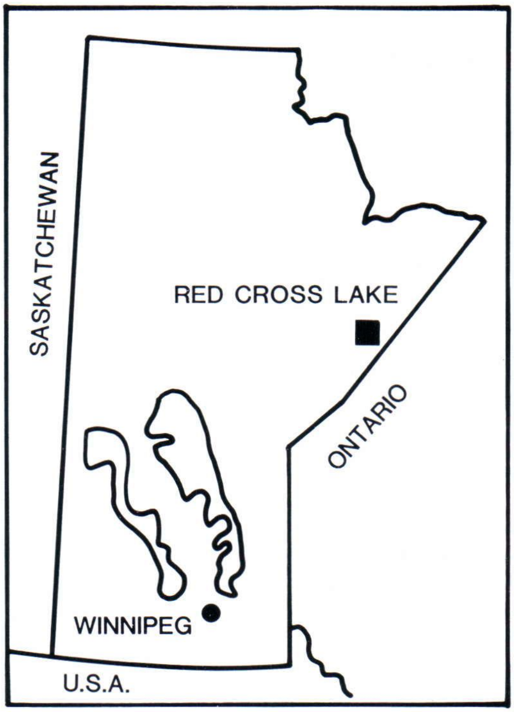

Fig. 1. Location of the Red Cross Lake pegmatite swarm in Manitoba.

The parent pegmatite

The examined rubidian microcline occurs in a pegmatite swarm outcropping on the northeastern shoreline of Red Cross Lake, northeastern Manitoba at about 92°48'W/55°05'N (Fig. 1). The pegmatites and adjacent pegmatitic granites are located in one of the E-W trending greenstone belts of the Sachigo subprovince, the northernmost crustal segment of the Archean Superior province of the Canadian Shield.

The pegmatite swarm consists of 17 dikes trending close to E—W and steeply dipping to the south. They are emplaced into pillowed metabasalts and volcaniclastic metasediments. The dikes occupy a fracture system about 55 m wide; individual pegmatites vary from a few centimetres to 3.5 metres in outcrop width. All pegmatites are extremely sheared, largely fine-grained, and banded to finely laminated in an off-white and pale purple color. The original texture and grain size are partly preserved only in rare lenticular relics within the sheared rock, or in local protrusions into the host rock that escaped the main deformation effects. It appears that the shearing affected mainly the pegmatites, leaving the adjacent wallrock much less disturbed.

The principal minerals constituting the pegmatites are albite, quartz, microcline and lithian muscovite ($2M_1$). Rubellite and lepidolite ($2M_2$) are subordinate; amblygonite, beryl (Jambor and Potter 1967) and pollucite (B. B. Bannatyne, pers. comm. 1980) occur in minor quantities. The paragenesis of the pegmatite dikes is undoubtedly more diversified, as indicated by elevated values of tantalum assays (D. L. Trueman, pers. comm. 1981), but no systematic examination of the pegmatites was undertaken to date.

The rubidian microcline

The rubidian microcline was found in the northern flank of one of the pegmatites located near the centre of the swarm, in a non-sheared, coarse-grained aggregate of quartz and K-feldspar that fills in a re-entrant angular notch in the wallrock. »Single-crystal« fragments of the rubidian microcline, showing somewhat deformed but continuous cleavage, were collected that reach 5 centimetres in maximum dimensions. The color of the microcline is dark grey to blackish grey, somewhat patchy in most samples. Two specimens designated RC—10A and RC—10B were selected for detailed examination.

Physical properties

Despite its dark color in hand specimen, the rubidian microcline is clean and free of alteration effects. Immersion liquid mounts reveal only local diffuse bands of dusty particles along the boundaries of perthitic albite with the K-phase matrix.

Numeric values of refractive indices, birefringence, 2V, extinction angles, characteristic infrared absorption bands and density are given in Table 1.

The rubidian microcline is partly grid-twinned and perthitic, but largely non-perthitic and forming simple contact Baveno twins of large individuals that reach 10 mm in size.

The perthitic type contains relatively coarse and irregular veinlets and patches of albite (5 to 10 vol.%). The veinlets show a tendency to be oriented parallel to the (110) and ($1\bar{1}0$) planes of the K-feldspar host. Dense lamellar twinning according to the Albite law is typical of all the perthitic albite; the twinning is oriented parallel to the Albite-twinned lamellae of the microcline phase. Refractive indices on the (001) cleavage fragments of albite compared to the data of Morse (1968) indicate a composition variable between $Ab_{97}An_3$ and $Ab_{95}An_5$. The potassic phase of the perthitic rubidian microcline shows widely variable patterns of grid twinning of »individual« crystals (»morphological units« of F. Laves) that are themselves subject to local Baveno twinning. In cleavage fragments parallel to (001), local patches with extremely regular cross-hatched twinning (chessboard type as shown in Fig. 1b of Fitzgerald and McLaren 1982) grade into areas of very irregular twinning

Table 1. Physical properties of the rubidian microclines.

	Red Cross Lake		Maximum microcline	
	RC-10A	RC-10B	$RbAlSi_3O_8$	$KAlSi_3O_8$
α	1.518—1.520	1.518—1.520	—	1.518[3]
β	1.522—1.523	1.522—1.524	—	1.522[3]
γ	1.525—1.526	1.525—1.526	—	1.525[3]
γ—α	0.007	0.006	—	0.007[3]
(—)2V	78°	76—80°	—	86.7°[4]
n̄ calc.	1.526	1.526	1.535[1]	1.526[5]
X' (001)	18—21°	19—21°	—	18°[6]
X' (010)	7—8°	7—8°	—	5°[7]
IR absorption A	15.455 μm	15.455 μm	—	see Fig. 1
IR absorption B	18.585 μm	18.585 μm	—	
D meas.	2.604(3)	2.612(3)	—	2.558[8]
D calc.	2.607	2.614	2.893[2]	2.557[9]

[1] based on the calculated density (see below), [2] based on V = 745.33Å³ (Pentinghaus and Henderson 1979, 1985), [3] Finney and Bailey (1964), Brown and Bailey (1964), [4] Su *et al.* (1984), [5] based on calculated density (see below), [6] Stewart (1975), [7] Winchell (1951), [8] synthetic (Orville 1967), [9] based on V = 722.60Å³ (Kroll and Ribbe 1983).

boundaries, wavy extinction and gross volume imbalance between the individual members of the lamellar twins. Textural relationships suggest recrystallization of the chessboard pattern, with preferential growth and coalescence of one set of lamellae at the expense of the other set (Černý and Macek 1972, 1974). In contrast, the extinction is fairly uniform throughout the twinned feldspar in sections parallel to (010).

The predominant non-perthitic type of the rubidian microcline contains sparse inclusions of randomly oriented platy albite (commonly up to 5 %, rarely 10 %). The platy albite commonly forms simple Albite twins. Individual crystals of the potassic phase combined in the Baveno twins seem to be optically monocrystalline individuals, with only a faint hint of undulatory extinction in some grains.

The mutual relationship between the grid-twinned perthitic and the Baveno-twinned non-perthitic types of the rubidian microcline is not evident from the available material. Gradual recrystallization of the former type into the latter one does not seem to be probable under static conditions, but a thorough recrystallization under stress leading to a different twinning style might deserve consideration. The parent veins certainly are among the most strained pegmatites ever examined.

The optical orientation of the microcline phase is triclinic, as demonstrated by the extinction angles on (001) and (010) (Table 1), and by the orientation of the cleavages and twinning planes relative to the axes of optical indicatrix as determined on the universal stage. The optical orientation is close to that of the maximum microcline shown on the Nikitin diagram by Fediuk (1961, Fig. 65). Similarly, the values of the optic axial angle, determined orthoscopically on the universal stage, are close to those of maximum microcline (Table 1).

Optical measurements of a Baveno-twinned rubidian microcline of the non-perthitic type established the angular relationships between the optical indicatrix, the Baveno twin contact plane and the cleavages and partings parallel to 001, 021, $\bar{1}\bar{1}1$ and 110 (in order of decreasing quality of morphological definition). The morphological data were checked against angular positions calculated from the unit cell dimensions (discussed in the following section). The mutual deviations of optically determined morphological data and their counterparts calculated from structural parameters did not exceed 2° for the most prominent elements, and they were less than 4° for the poor parting tracks of ($\bar{1}\bar{1}1$). Unit cell dimensions were also used for calculation of [001], ⊥ (010), and ⊥ [001]//(010) poles. The integrated morphological, optical and structural data shown in Figure 2 lead to the Euler angle values $\Phi = +74°$, $\Psi = 95.5°$ and $\Theta = 72.5°$.

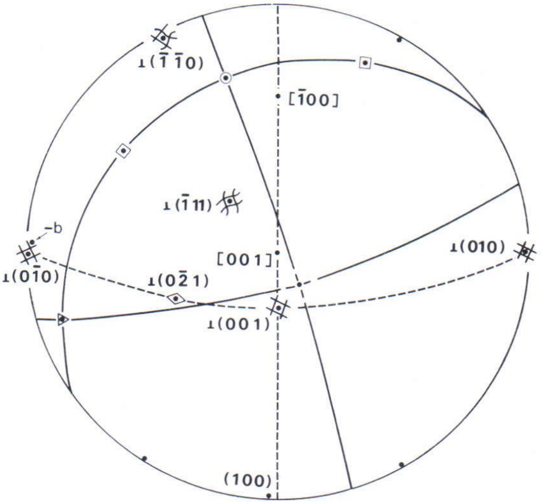

Fig. 2. Stereographic projection (upper hemisphere) of the optical, morphological, and structural crystallography of the non-perthitic, Baveno-twinned rubidian microcline. See text for details.

The refractive indices determined in Na light, by immersion on universal stage, are somewhat variable but on average higher than literature data for Fe- and Rb-poor microcline (Table 1). Densities also are high, determined on a Berman torsion balance with toluene as the displacement liquid.

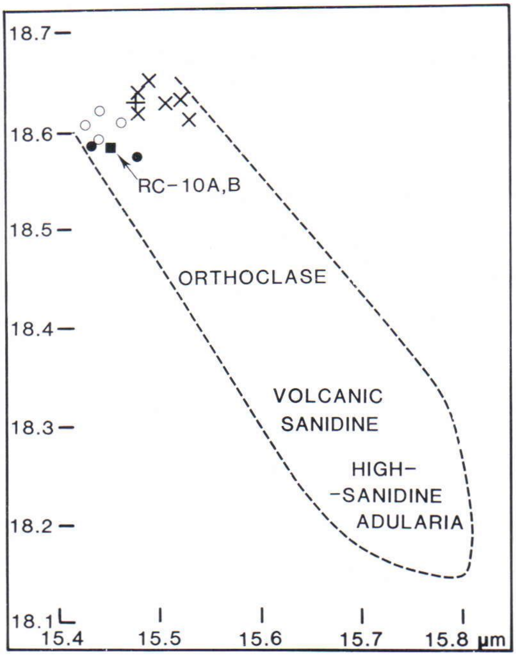

Fig. 3. Plot of the characteristic infrared absorption bands of K-feldspars in the 15—16 µm and 18—19 µm regions. X — microclines of Hafner and Laves (1957); open circles — microclines of Lehtinen (1974); + — microcline of Akizuki and Sunagawa (1978); solid dots — microclines of Černý and Chapman (1984); solid square — rubidian microclines from Red Cross Lake (overlapping one solid dot). The general regions of other feldspar types are shown as established in the above references.

Infrared absorption spectra were collected between 14.9 and 19.3 µm on pellets prepared from a mixture of 0.22 g KBr and 0.0006 g of the feldspar. The spectra were recorded on the Nicolet MX-1 Fourier-transform IR spectrometer, calibrated by laser interferometry and checked with an international polystyrene standard. The wavelengths of two characteristic absorption bands located in the regions of 15—16 and 18—19 µm (A and B absorptions, respectively, of Hafner and Laves 1957, Figs. 2b and 3, and Laves and Hafner 1962, Figs. 1 to 3) are closely comparable to those determined for other microclines (Fig. 3).

Structural characteristics

Initial X-ray powder diffractograms showed the examined microcline to possess a high and homogeneous triclinicity variable from 0.90 to 0.95 in different samples. A departure of most diffraction peaks from the typical 2Θ values of microcline was also noticeable, but no difference was found between the grid-twinned and Baveno-twinned types. Unit cell dimensions of the two selected specimens were refined from data re-

Table 2. Unit cell dimensions of the rubidian microclines.

	a(Å)	b(Å)	c(Å)	α(°)	β(°)	γ(°)	V(Å^3)	n[1]
Max. K-microcline S & W[2]	8.597	12.964	7.222	90.637	115.933	87.683	723.24	
Max. K-microcline S[3]	8.5903	12.9659	7.2224	90.65	115.96	87.65	722.62	
Max. K-microcline F[4]	8.582(5)	12.965(5)	7.222(5)	90.63(2)	115.94(2)	87.68(2)		
Max. K-microcline K & R[5]	8.592	12.962	7.222	90.62	115.95	87.67	722.60	
RC-10BKex.[6]	8.6360(14)	12.9682(9)	7.2232(11)	90.595(7)	116.006(9)	87.830(8)	726.50(25)	42
RC-10A	8.6352(6)	12.9690(5)	7.2248(5)	90.575(5)	116.002(4)	87.894(4)	726.70(11)	83
RC-10B	8.6373(7)	12.9691(5)	7.2264(6)	90.588(5)	116.002(5)	87.842(5)	727.01(13)	85
Max. Rb-microcline P & H[7]	8.8399(9)	12.9619(8)	7.2515(9)	90.521(7)	116.158(6)	88.012(6)	745.33(18)	
Max. Rb-microcline McM[8]	8.843(2)	12.961(2)	7.256(2)	90.53(1)	116.20(1)	88.01(1)	745.7(4)	

[1] number of diffractions used in unit cell refinement

[2] Stewart and Wright (1974), extrapolated

[3] Smith (1974a), extrapolated

[4] Ferguson (1980), extrapolated

[5] Kroll and Ribbe (1983), extrapolated

[6] K-exchanged

[7] Pentinghaus and Henderson (1979, 1985)

[8] McMillan *et al.* (1980), 92.76 mol.% Rb-feldspar

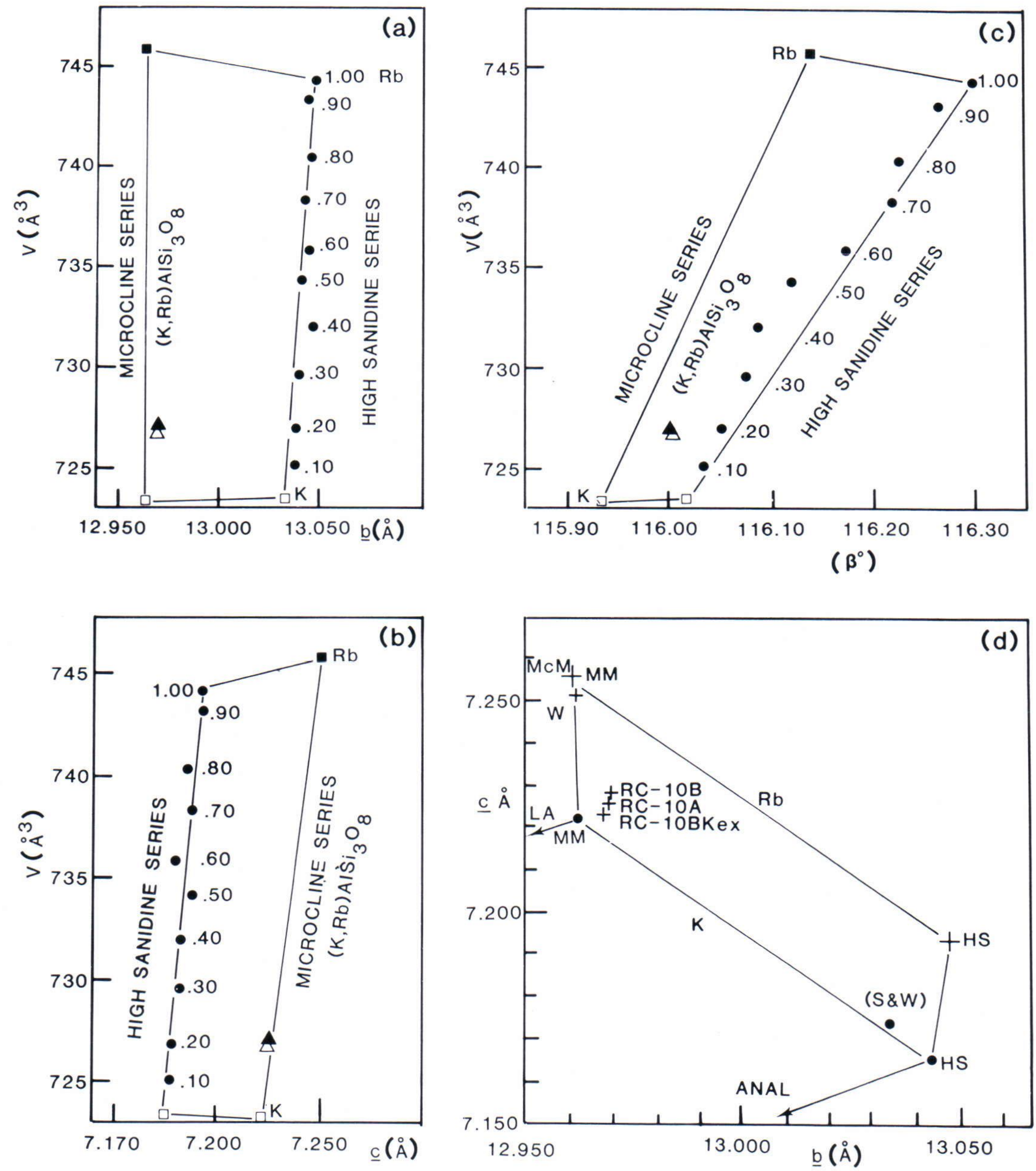

Fig. 4. (a, b, c) Position of the RC-10A (open triangle) and RC-10B (solid triangle) rubidian microclines in the unit cell volume vs. b, c, and β diagrams of Pentinghaus and Henderson (1984) for the ordered and disordered K-Rb feldspars; open squares — data from Stewart and Wright (1974); solid square — Weitze (1971); solid dots — Pentinghaus and Henderson (1979, 1984). (d) The rubidian microclines in the expanded b-c plot; potassic MM and HS after Kroll and Ribbe (1983) and Kroll (pers. comm. 1983), respectively, with HS of Stewart and Wright (1974) shown for comparison (S & W); rubidian HS from Pentinghaus and Henderson (1979, 1984; PH) and rubidian MM from McMillan *et al.* (1980; McM) and Weitze (1971; W). Crosses indicate ± 1σ.

corded in an AEG Guinier-Jagodzinski camera, using the CuKα_1 radiation. Specpure NBS-standard silicon (99.999 %; a = 5.43054 Å at 25°C) was selected as internal standard. The mean error in reading the film record was estimated at ±0.02 mm, *i.e.* ±0.01°2Θ. The resulting data are listed in Table 2 in comparison with the unit cell dimensions of end-member potassic and rubidian maximum microclines.

Figure 4 shows the unit cell dimensions plotted on the b vs. V, c vs. V and β vs. V diagrams of Pentinghaus and Henderson (1979, 1984), and on the modified b—c plot of Wright and Stewart (1968), extended to cover the field of Rb-feldspars. In Figure 4a, b, and c, the potassic end-members are taken from Stewart and Wright (1974). Figure 4d is plotted using the potassic end-members of Kroll and Ribbe (1983 for MM, pers. comm. 1983 for HS).

All diagrams indicate that the Rb-feldspar component in the potassic phase of the examined feldspars is close to 20 mol.%. The structural state is indicated as close to that of maximum microcline, in accordance with the triclinicity values quoted above. The only deviation is shown by β which suggests an intermediate structural state.

Cation exchange was performed on the specimen RC-10B to compare its structural state with K-based feldspars. A Na-feldspar was obtained first by cation exchange with molten NaCl (NaCl/feldspar = 100/l) at 828°C for 6 hours. Excess chlorides were dissolved from the resulting phase with 300 ml HCl (1 : 2), and the feldspar was subsequently treated in molten KCl (KCl/feldspar = 50/l) at 830°C for 5 hours. Unit cell dimensions of this final feldspar phase are given in Table 2 under the sample designation RC-10BKex. It is noteworthy that in Figure 4d this K-based feldspar plots only about halfway between the natural rubidian microcline and the potassic maximum microcline-high sanidine boundary. It would plot very close to the natural phases in Figure 4a, b, c; the data are not plotted in these diagrams to avoid an additional overlap of symbols.

Chemical compositions

Results of chemical analyses, atomic contents, end-member feldspar contents and geochemically significant ratios of the alkali metals are summarized in Table 3.

Chemical analysis was performed in the Laboratoire de Géochimie Analytique, École Polytechnique in Montreal by Mr. V. Kubat. SiO_2 and Al_2O_3 were determined by X-ray fluorescence spectrometry, and Fe_2O_3, CaO, Li_2O, Na_2O, K_2O, Rb_2O, and Cs_2O by atomic absorption spectrophotometry. A modification of Fratta's (1974) atomic absorption technique was used for Tl_2O. Replicate analyses for SiO_2 and Al_2O_3 were run at the Department of Earth Sciences, University of Manitoba and at the Department of Geology, University of Ottawa. Electron microprobe checks of the K-feldspar phase for P, Ba and Sr were negative, indicating concentrations below 0.1 wt.%.

X-ray diffraction patterns and optical checks of the analyzed material RC-10A indicated a pure feldspar composition but those of RC-10B revealed a small admixture of quartz. Comparison with calibrated K-feldspar + quartz mixtures indicated the quartz level at 4±1 wt.%. Subtraction of this amount of SiO_2 from the analysis and recalculation to 100 wt.% gave a composition with satisfactory stoichiometry (Table 3).

The bulk compositions of the two perthitic feldspars were recalculated to a close approximation of their K-feldspar components, using the Na_2O contents of the potassic phases as determined by electron microprobe. K, Rb, Cs and Tl were assumed to be retained in the K-phase of the perthite (see, *e.g.*, Heier and Taylor 1959 and Smith 1974b for data relevant to partitioning coefficients).

The contents of CaO were divided between the perthitic and/or platy albite and (Ab + An) in solid solution proportionally to the allotment of

Na_2O. This arbitrary procedure may have introduced a slight error because some of the CaO may be present as carbonate; rare microscopic films of carbonate have been identified optically, and the Na/Ca ratios are lower than expected for the optically determined composition of perthitic and platy albite. Also, the subtraction of stoichiometric (Ab + An) increases the Si/Al ratio in both feldspars, suggesting that some Ca may be bound in the Schwantke's molecule rather than the anorthite component. However, the quantities involved are trivial, bordering on the limit of analytical precision and consequently inadequate for interpreting the substitution mechanism. The effect of any error on the calculated composition of the K-phases would be negligible.

The Li content was arbitrarily assigned to the K-feldspar component. The crystallochemical role of Li in K-feldspars is uncertain, and may be related to local lattice deformation (Iiyama and Volfinger 1976). In co-existing feldspars, empirical data indicate preferential partitioning of Li into plagioclase (as reviewed by Smith 1974b). However, ion microprobe studies of pegmatitic perthites indicate strong partitioning of Li into the potassic phase (Mason 1980, 1982).

The data of Table 3 show that the K-feldspar phase of the samples RC-10A and RC-10B contains 15.7 and 18.4 mol.% of the Rb-feldspar

Table 3. Chemical composition of the rubidian microclines.

	RC-10A, wt.%		RC-10B, wt.%		
	perthite[1]	K-phase[2]	orig.[3]	perthite[1, 4]	K-phase[2]
SiO_2	65.33	63.26	65.18	63.49	63.17
Al_2O_3	17.93	17.70	17.05	17.70	17.53
Fe_2O_3	0.07	0.07	0.08	0.08	0.09
CaO	0.18	0.06	0.07	0.07	0.03
Li_2O	0.05	0.05	0.09	0.09	0.10
Na_2O	1.16	0.42	1.18	1.22	0.41
K_2O	12.00	12.91	10.99	11.41	12.28
Rb_2O	4.70	5.06	5.25	5.45	5.87
Cs_2O	0.40	0.43	0.43	0.45	0.48
Tl_2O	0.0367	0.0395	0.0407	0.0418	0.0450
	100.08[6]	100.00	100.34	100.00	100.00
K/Rb	2.32			1.90	
K/Cs	26.4			22.4	
K/Tl	282			236	
Rb/Cs	11.4			11.8	
Rb/Tl	122			124	

	RC-10A, at. cont.[5]		RC-10B, at. cont.[5]	
	perthite	K-phase	perthite	K-phase
Si	5.998	6.010	6.014	6.020
Al	1.994	1.981	1.976	1.968
Fe^{3+}	0.005	0.005	0.006	0.006
Σ	1.999	1.986	1.989	1.974
Ca	0.018	0.006	0.007	0.003
Li	0.019	0.019	0.034	0.038
Na	0.213	0.077	0.224	0.076
K	1.444	1.564	1.378	1.493
Rb	0.285	0.309	0.331	0.359
Cs	0.016	0.017	0.018	0.019
Tl	0.001	0.001	0.001	0.001
Σ	1.996	1.993	1.993	1.989
Σ cat.	9.993	9.989	9.996	9.983
Or[7]	73.04	79.24	70.34	76.53
Ab	10.77	3.90	11.43	3.90
An	0.91	0.30	0.36	0.15
Rb-f	14.42	15.65	16.90	18.40
Cs-f	0.81	0.86	0.92	0.97
Tl-f	0.05	0.05	0.05	0.05
Σ	100.00	100.00	100.00	100.00

[1] chemical composition of rubidian microcline-perthite, as analyzed

[2] chemical composition of the K-phase of the perthite, based on Na_2O by electron microprobe and arbitrary proportional splitting of CaO between plagioclase in solid solution and perthite albite; Li_2O, Rb_2O, Cs_2O and Tl_2O assigned to the K-phase

[3] original analysis of a quartz-contaminated sample

[4] corrected by subtraction of 4 wt.% quartz

[5] normalized to 16 oxygens

[6] includes 0.004 MnO

[7] mol.%

component, respectively. These data are in good agreement with the estimates based on structural parameters (Fig. 4), particularly because the Cs and Tl contents can be expected to exert structural effects similar to those of Rb. The combined contents of (Rb, Cs, Tl)-feldspars in the two samples are 16.6 and 19.4 mol.%, respectively.

Discussion

Several compositional and structural relationships in the described feldspars deserve comment because of their general significance for the crystal chemistry of rubidian K-feldspars, and for their mode of occurrence in granitic pegmatites.

Rare-alkali enrichment

As stated in the introduction, the Rb-content of sample RC-10B (49,800 ppm) is the highest ever encountered in a natural K-feldspar. The Cs content (4240 ppm) may be among the highest as well, considering the fact that most of the data showing $Cs_2O > 0.4$ wt.% are rather old and of low accuracy (e.g., Adamson 1942). The Tl content of RC—10B (402 ppm) is also unsurpassed in the available literature.

The fractionation ratios K/Rb and K/Cs are the most extreme ever encountered in K-feldspar (Table 3). They are exceeded only in lepidolites (*cf.* Černý 1982 for a review of Rb and Cs in micas). However, the Rb/Tl ratio reconfirms the close geochemical similarity of these two elements. It is well within the range of 300—65 which is considered typical of terrestrial igneous rocks (Shaw 1957, de Albuquerque and Shaw 1972). Exceptionally low Rb/Tl ratios were reported only from the pegmatites of Kola Peninsula (Borovik-Romanova and Sosedko 1960); they may result from a regional Tl anomaly or from an analytical problem.

It is not surprizing that the described feldspars occur in pollucite-bearing rare-element pegmatites that have been already known for their Rb-rich micas, and for the high contents of the rare alkali metals in their bulk compositions (Jambor and Potter 1967). A systematic mineralogical study of these pegmatites is desirable because the fractionation of other geochemically related element pairs (such as Nb—Ta, Zr—Hf, Al—Ga et sim.) may also reach extreme levels.

Rb content and optical properties

The only attempt at a systematic study of physical properties of Rb-enriched microcline is that of Gordiyenko (1964). However, his samples were restricted to $Rb_2O < 1.5$ wt.%, and the optical properties were determined, by Gordiyenko's own admission, with insufficient accuracy. Thus there is virtually no information available for comparison with the data of Table 1 and Figure 2.

Although a general match between the optics of maximum K-microcline and our rubidian microclines is evident, some deviations can be observed in the quantitative values of individual properties. For example, extinction on (001) reaches 21°, similar to the 20° reported by Adamson (1942) for the Rb-enriched feldspars from Varuträsk. The extinction angle of a K-based maximum microcline is quoted as 18° (Stewart 1975). The extinction angle of 7—8° on (010) is appreciably larger than the »textbook« value of 5° (*e.g.*, Winchell 1951).

The refractive indices calculated using Mandarino's (1976) specific refractive energy values seem to be indicative of γ rather than $\bar{n}$ $(= (\alpha + \beta + \gamma/3)$. This is suggested not only by the comparison of calculated and measured values for maximum K-microcline and the RC samples, but also by the calculation for end-member low albite which gives $\bar{n} = 1.539$ (identical to measured γ; *cf.* Smith 1974a, p. 386). Thus it is probable that the major cause for the discrepancy is in the *k*-value of SiO_2 and/or Al_2O_3 rather than in those of the alkali oxides.

Nevertheless, the calculated values of n̄ seem to be shifted uniformly for all feldspars considered here, and the relatively narrow range of refractive indices between the K-based and Rb-based maximum microclines appears to be real.

As shown in Figure 3, the characteristic A and B bands in the IR absorption spectra of the RC—10 feldspars do not differ from their counterparts generated by (Rb, Cs)-poor microclines. According to Iishi *et al.* (1971) and Lehtinen (1974), the B band of microcline results from coupling of O—Si—O bending and K—O stretching vibrations. Figure 3 indicates that the (Rb, Cs, Tl) substitution of about 20 at.% K does not affect the position of the B absorption peak.

Composition and structural parameters

The chemical composition and unit cell dimensions of the examined feldspars are in good mutual agreement when compared to the grids of Figure 4. However, it should be noted that at least the K-rich part of the high-sanidine K—Rb series of Pentinghaus and Henderson (1979, 1984) does not represent a full (Si, Al) disorder. More extreme unit cell dimensions were recently extrapolated for pure K-based high sanidine (Ferguson 1980, Kroll and Ribbe 1983, Kroll pers. comm. 1983) and discovered in some pegmatitic adularias (Černý and Chapman 1984). It is also noteworthy that the maximum Rb-microcline is represented by two sets of data in Table 2 and Figure 4d (Pentinghaus and Henderson 1979 and 1984, McMillan *et al.* 1980). However, the difference is minimal, caused largely by the c dimension and showing an overlap of 2σ's even for this parameter. Unit cell volumes of these two feldspars are statistically identical, within ±1σ.

Rb content and ordering

Gordiyenko and Kamentsev (1967) and Karnin (1980) concluded that the large size of the Rb^+ cation prevents Rb-rich feldspars from extensive ordering, and arrests the process at the monoclinic orthoclase stage. These conclusions, based on studies of territorially limited sample suites, were refuted by Černý and Macek (1972), Martin (1982) and others who described near-maximum microclines with Rb contents matching or exceeding those of the feldspars studied by Gordiyenko and Kamentsev. The recent syntheses of end-member maximum Rb-microclines have also shown that highly ordered feldspar framework can accommodate Rb as the dominant cation.

Afonina *et al.* (1979) examined Rb-enriched K-feldspars from three pegmatite fields and concluded that Rb and Cs do retard ordering of K-feldspars but their influence can largely be overcome by other factors such as high P of crystallization or late deformation (Fig. 5). This conclusion is strengthened by the fact that near-maximum microclines with 2.5 to 5.1 wt.% $(Rb, Cs)_2O$ are also found in undeformed and relatively shallow-seated pegmatites (Fig. 5; Varuträsk-Adamson 1942, Tanco and Lower Tanco—Černý and Macek 1972, Ferreira 1984). This compositional-cum-structural range was not represented in the study of Afonina *et al.* (1979). Also, structural states variable from monoclinic orthoclase to maximum microcline (triclinicity 0.98) are known to evolve in a single pegmatite in feldspars that show nearly uniform (Rb, Cs) contents (Fig. 5; Černý and Macek 1974). Differences in composition, distribution and interaction time of late fluids reacting with the feldspars may primarily be responsible for the variable structural state in these pegmatites.

The above evidence indicates that various factors promoting the (Si, Al) ordering in alkali feldspars (Martin 1974) can and do easily override the retarding effect of Rb and Cs. Highly rubidian near-maximum microcline is far from exceptional, and the present data expand its compositional range to 5.90 wt.% $(Rb, Cs)_2O$ (although deformation may be a significant or-

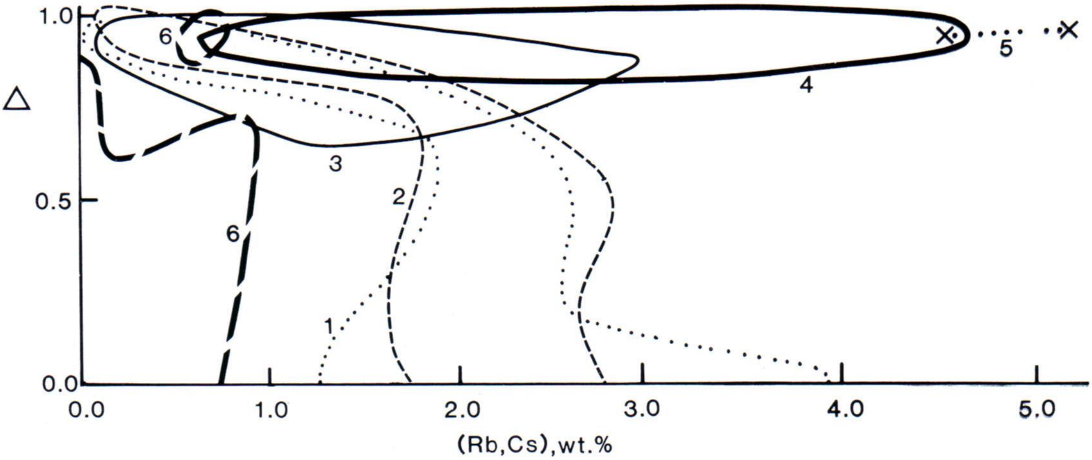

Fig. 5. Triclinicity (Δ) vs. (Rb, Cs)$_2$O content of K-feldspar; 1) rare-element pegmatites of a »European part of the USSR« with well expressed textural and compositional zoning, 22 samples; 2) rare-element albite-rich pegmatites of »one of the Siberian fields«, 19 samples; 3) rare-element spodumene-bearing pegmatites of »another pegmatite field in Siberia«, texturally homogeneous, 20 samples (1 to 3 from Afonina *et al.* 1979); 4) the Tanco and Lower Tanco pegmatites, southeastern Manitoba, 101 samples (Černý and Macek 1972, Ferreira 1984, unpubl. data of P. Č.); 5) this study; 6) lepidolite-bearing pegmatite at Radkovice, Czechoslovakia, 19 samples (Černý and Macek 1974).

dering factor in this case, in accord with the reasoning of Afonina et al. 1979).

It is noteworthy that Pentinghaus and Henderson (1979, 1984) interpret the maximum Rb-microcline as a metastable phase, as its unit cell volume (745.5 Å^3) is greater than that of its high-sanidine counterpart (744.3 Å^3). A plot of unit cell volumes of maximum K-Rb microclines (McMillan *et al.* 1980) and high Rb-sanidines (Pentinghaus and Henderson 1979, 1984) against their Rb-feldspar contents shows that the above argument applies to the range of 100 to about 20 mol.% Rb-feldspar. The latter value is very close to the (Rb, Cs, Tl) -feldspar content of sample RC—10B, 19.4 mol.%.

Rb content and triclinicity

Lopes Nunes (1973) noticed that in the pegmatites of the Alto Ligonha region in Mozambique, the highest Rb contents are found in structurally heterogeneous feldspar samples with highly triclinic and monoclinic components. The same observation was made by McGregor (1984) who re-examined pegmatite feldspars studied previously by Ucakuwun (1981) from the Dryden area in north-western Ontario. McGregor also found, by single crystal methods, that the quasi-monoclinic peaks in the powder patterns of the Dryden feldspars (interpreted as orthoclase diffractions by Ucakuwun) actually belong to an intermediate microcline of very low triclinicity. In the Alto Ligonha and Dryden areas, the structurally heterogeneous K-feldspars are found together with homogeneous (and highly ordered) feldspars in the intermediate and core-margin zones of the pegmatites.

In the Tanco pegmatite, the singular highest Rb content (3.61 wt.% Rb$_2$O) was also found in a K-feldspar of mixed triclinic and (quasi-) monoclinic structural state (Černý and Simpson 1978). However, in this case the structurally heterogeneous feldspar belongs to a late generation veining pollucite bodies, and other samples of this feldspar type have much lower Rb contents (Černý and Simpson 1978, unpubl. data of P. Č.). The primary blocky K-feldspars of the Tanco pegmatite have Rb contents of 0.80 to 2.90 wt.% Rb_2O and homogeneous triclinicity (0.85—0.96 in different samples). The Varuträsk pegmatite may show similar relationships (Adamson 1942, Quensel 1956).

In other localities, the highest Rb contents within a given pegmatite are found in primary, structurally homogeneous K-feldspars. This is, for example, the case of the Lower Tanco pegmatite (Ferreira 1984), Kola Peninsula (Gordiyenko and Kamentsev 1967), Mongolian Altai No. 3 (Solodov 1960, Wang *et al.* 1981), and it also seems to be true for the Red Cross Lake pegmatites.

On the face of the available evidence, it is unlikely that a particularly high concentration of Rb may be typical of specific structural states of K-feldspar. Incorporation of Rb into the K-feldspars crystallizing at different stages of the pegmatite consolidation can hardly be expected to correlate with order-disorder relationships that are largely a post-crystallization effect (unless an extensive role of feldspar recrystallization and Rb migration is invoked). Such a conclusion is also in agreement with the interpretation reached in the preceding section. However, the present data base is rather narrow, and further research is desirable into the relationships between the chemistry, structural state, structural homogeneity and paragenetic position of pegmatitic K-feldspars, including their response to late metasomatic processes and crystallization.

Acknowledgements. Our thanks are due to Dr. D. L. Trueman and J. S. D. Parker, and to the Tantalum Mining Corporation of Canada, Ltd. for support and guidance in the field. Messrs. M. A. Wise and L. Chackowsky provided the preliminary X-ray powder diffraction data. Dr. G. Perrault and Mr. V. Kubat (École Polytechnique, Montreal) performed the chemical analyses with exemplary care. Dr. B. R. Henry and Mr. W. Buchannon (Department of Chemistry, University of Manitoba) made the services of their IR laboratory available and collected the spectra, respectively. The study was supported by the NSERC Operating Grant A7948 to P. Č.

References

Adamson, O. J., 1942. Minerals of the Varuträsk pegmatite. XXXI. The feldspar group. Geol. Fören. Förh. 64, 19—54.

Afonina, G. G.; Makagon, V. M.; Smakin, B. M.; Glebov, M. P. & Makrygin, A. I., 1979. Effects of rubidium and cesium on the structural states of potash feldspars from rare-metal pegmatites. Internat. Geology Rev. 21, 597—604.

Akizuki, M. & Sunagawa, I., 1978. Study of the sector structure in adularia by means of optical microscopy, infrared absorption, and electron microscopy. Mineral. Mag. 42, 453—462.

Albuquerque, C. A. R. de & Shaw, D. M., 1972. Thallium. Handbook of Geochemistry, V. II/3, Springer-Verlag, Berlin.

Anderson, A. J., 1984. The Cross Lake pegmatite field, Manitoba. M.Sc. thesis, University of Manitoba, Winnipeg, 251 pp.

Borovik-Romanova, T. F. & Sosedko, A. F., 1960. Relation between thallium and rubidium in minerals from pegmatite veins of the Kola Peninsula. Geochemistry 1960, 34—42.

Brown, B. E. & Bailey, S. W., 1964. The structure of maximum microcline. Acta Cryst. 17, 1391—1400.

Černý, P., 1982b. Mineralogy of rubidium and cesium. MAC Short Course Handbook 8, 149—162.

— *& Chapman, R.,* 1984. Paragenesis, chemistry and structural state of adularia from granitic pegmatites. Bull. Minéralogie 107, 369—384.

— *& Macek, J.,* 1972. The Tanco pegmatite at Bernic Lake, Manitoba. V, Coloured potassium feldspars. Canad. Mineral. 11, 679—689.

— *& Macek, J.,* 1974. Petrology of potassium feldspars in two lithium-bearing pegmatites. *In:* The Feldspars, Proc. NATO Adv. Study Inst. Manchester 1972, Manchester University Press, 615—628.

— *; Trueman, D. L.; Ziehlke, D. V.; Goad, B. E. & Paul, B. J.,* 1981. The Cat Lake-Winnipeg River and the Wekusko Lake pegmatite fields, Manitoba. Man. Mineral Res. Div. Econ. Geol. Rept. ER80—1, 240 p.

Fediuk, F., 1961. Fjodorovova mikroskopická metoda (Fjodorov's microscopic method); in Czech, NČSAV Prague, 185 p.

Ferguson, R. B., 1980. From unit cell parameters to Si/Al distribution in K-feldspars. Canad. Mineral. 18, 443—458.

Ferreira, K. J., 1984. The mineralogy and geochemistry of the Lower Tanco pegmatite, Bernic Lake, Manitoba, Canada. Unpubl. M.Sc. thesis, Univ. of Manitoba, 239 p.

Finney, J. J. & Bailey, S. W., 1964. Crystal structure of an authigenic maximum microcline. Zeits. Krist. 119, 413—436.

Fitzgerald, J. D. & McLaren, A. C., 1982. The microstructures of microcline from some granitic rocks and pegmatites. Contrib. Mineral. Petrol. 80, 219—229.

Foord, E. E., 1976. Mineralogy and petrogenesis of layered pegmatite-aplite dikes in the Mesa Grande district, San Diego County, California. Unpubl. Ph.D. thesis, Stanford Univ., 326 p.

Fratta, M., 1974. AAS determination of ppb amounts of thallium in silicate rocks. Canad. Journ. Spectroscopy 19, 33—37.

Gordiyenko, V. V., 1964. On rubidium microcline from pegmatite veins of the sodium-lithium type. Zapiski Vses. Min. Obsh. 93, 281—288 (in Russian).

— *& Kamentsev, I. E.*, 1967. On the nature of the rubidium admixture in potassic feldspar. Geokhimiya 1967, 478—481 (in Russian).

Hafner, S. & Laves, F., 1957. Ordnung/Unordnung und Ultrarot-Absorption. II. Variation der Lage und Intensität einiger Absorptionen von Feldspäten. Zur Struktur von Orthoklas und Adular. Zeits. Krist. 103, 204—225.

Heier, K. S., 1962. Trace elements in feldspars — a review. Norsk Geol. Tiddskrift 42, 415—454.

— *& Taylor, S. R.*, 1959. Distribution of Li, Na, K, Rb, Cs, Pb and Tl in southern Norwegian pre-Cambrian alkali feldspars. Geochim. Cosmochim. Acta 15, 284—304.

Iishi, K.; Tomisaka, T.; Kato, T. & Umegaki, Y., 1971. Isomorphous substitution and infrared and far infrared spectra of the feldspar group. Neues Jahrb. Mineral., Abh. 115, 98—119.

Iiyama, J. T. & Volfinger, M., 1976. A model for trace-element distribution in silicate structures. Mineral. Mag. 40, 555—564.

Jambor, J. L. & Potter, R. R., 1967. Rubidium-bearing dykes, Gods River area, Manitoba, G. S. C. Paper 67—15, 7 p.

Karnin, W.—D., 1980. Petrographic and geochemical investigations on the Tsaobismund pegmatite dyke, South West Africa/Namibia. Neues Jahrb. Mineral., Monatsh., 193—205.

Kroll, H. & Ribbe, P. H., 1983. Lattice parameters, composition and Al, Si order in alkali feldspars. Reviews in Mineralogy, 2, Feldspar Mineralogy, 2nd ed., Mineral. Soc. America, 57—99.

Laves, F. & Hafner, S., 1962. Infrared absorption effects, nuclear magnetic resonance and structure of feldspars. Norsk Geol. Tiddskr. 42, 57—71.

Lehtinen, M., 1974. Degree of Al/Si order in potassium feldspars. A combination of X-ray and infrared data. Contrib. Mineral. Petrol. 47, 223—230.

Lopes Nunes, J. E., 1973. Contribution a l'étude minéralogique et geochimique des pegmatites du Mozambique. Sci. de la Terre Nancy, Mem. 26, 261 p.

Mandarino, J. A., 1976. The Gladstone-Dale relationship — Part 1: Derivation of new constants. Canad. Mineral. 14, 498—502.

Martin, R. F., 1974. Controls of ordering and subsolidus phase relations in the alkali feldspars. *In:* W. S. MacKenzie and J. Zussman, eds., Proc. NATO Adv. St. Inst., Manchester Univ. Press, Manchester, England, 313—336.

— 1982. Quartz and the feldspars. Mineral. Assoc. Canada Short Course Handbook 8, 41—62.

Mason, R. A., 1980. Trace elements in alkali feldspars and element distribution in a perthite by ion probe microanalysis. 1980 Ann. Meet. GSA—MSA Abstr. w. Progr. 12, no. 7, 477.

— 1982. Trace element distributions between the perthite phases of alkali feldspars from pegmatites. Mineral. Mag. 45, 101—106.

McGregor, C. R., 1984. Characterization of granitic and pegmatitic feldspars from Lac du Bonnet, southeastern Manitoba and Dryden, northwestern Ontario by rapid X-ray diffraction and chemical methods. Unpubl. M.Sc. thesis, Univ. of Manitoba, 212 p.

McLaren, A. C., 1983. The microstructures of microclines. NATO Adv. Study Inst. on Feldspars and Feldspathoids Rennes, Progr. Abstr., 36—40.

McMillan, P. F.; Brown, W. L. & Openshaw, R. E., 1980. The unit cell parameters of an ordered K—Rb alkali feldspar series. Amer. Mineral. 65, 458—464.

Morse, S. A., 1968. Revised dispersion method for low plagioclase. Amer. Mineral. 53, 105—115.

Pentinghaus, H. & Henderson, C. M. B., 1979. Rubidiumaluminosilikat-Feldspat Rb(AlSi$_3$O$_8$); Stabilität, strukturelle Zustande und Schmelzverhalten: chemische und thermische Ausdehnung des (AlSi$_3$O$_8$)-Gerüstes. Fortschr: Mineral. 57, Beiheft 1, 119—120.

— *& Henderson, C. M. B.*, 1985. On Rb—feldspar RbAlSi$_3$O$_8$. (ms. in prep.).

Quensel, P., 1956. The paragenesis of the Varuträsk pegmatite, including a review of its mineral assemblage. Ark. Min. Geol. 2, 9—126.

Shaw, D. M., 1957. The geochemistry of gallium, indium, thallium — a review. Phys. Chem. Earth 2, 164—211.

Smith, J. V., 1974a. Feldspar Minerals. 1. Crystal Structure and Physical Properties. Springer-Verlag, New York.

— 1974b. Feldspar Minerals. 2. Chemical and Textural

Properties. Springer—Verlag, New York.

Solodov, N. A., 1960. Distribution of alkali elements and beryllium in minerals of one of the zoned pegmatites of Mongolian Altai. Geokhimiya 1960, 726—735. (in Russian).

Stewart, D. B., 1975. Optical properties of alkali feldspars. Mineral. Soc. America Short Course Notes 2, St23—St30.

— *& Wright, T. L.*, 1974. Al/Si order and symmetry of natural potassic feldspars, and the relationship of strained cell parameters to bulk composition. Bull. Soc. franç. Minéral. Crist. 97, 356—377.

Su, S. C.; Bloss, F. D.; Ribbe, P. H. & Stewart, D. B., 1984. Optic axial angle, a precise measure of Al, Si ordering in T_1 tetrahedral sites of K-rich alkali feldspars. Amer. Mineral. 69, 440—448.

Ucakuwun, E. K., 1981. The pegmatites and the granitoid rocks of the Dryden area, northwestern Ontario. Unpubl. M.Sc. thesis, Dept. Earth Sci., Univ. Manitoba, 152 p.

Wang, X.-J.; Zou, T.-R.; Xu, J.-G.; Yu, X.-Y., & Qiu, Y.-Z., 1981. Study of pegmatite minerals from the Altai region. Sci. Publ. House Beijing, 140 p. (in Chinese).

Weitze, R., 1971. Rubidiumeinbau in Tief-Plagioklasen. Unpubl. thesis, Technical University Hannover.

Winchell, A. N., 1951. Elements of optical mineralogy. 4th ed., Pt. II, Wiley New York.

Wright, T. L. & Stewart, D. B., 1968. X-ray and optical study of alkali feldspar: I. Determination of composition and structural state from refined unit cell parameters and 2V. Amer. Mineral. 53, 38—87.